scientific data

Check for updates

OPEN

DATA DESCRIPTOR

Genome-wide identification of accessible chromatin regions by ATAC-seq upon induction of the transcription factor bZIP11 in Arabidopsis

Alicia M. Hellens[1,2] ✉, Jazmine L. Humphreys[1,2,3], Franziska Fichtner[1,2,4], Miloš Tanurdžić[1,2], Christine A. Beveridge[1,2] & François F. Barbier[1,2] ✉

Basic leucine zipper 11 (bZIP11) is a transcription factor that is activated under low energy conditions in plants and plays a crucial role in enabling plants to adapt to starvation situations. Although previous results indicate that bZIP11 regulates chromatin accessibility based on evidence obtained from single genomic loci, to what extent this transcription factor regulates the chromatin landscape at the whole genome level remains unknown. Here we addressed this by performing an ATAC-seq (Assay for Transposase-Accessible Chromatin with high-throughput sequencing) on *Arabidopsis thaliana* (Arabidopsis) leaf protoplasts to obtain a profile of chromatin patterning in response upon bZIP11 induction. We identified, on average, 10,000 differentially accessible regions upon bZIP11 induction, corresponding to over 8,420 different genes out of the 25,000 genes present in the Arabidopsis genome. Our study provides a resource for understanding how bZIP11 regulates the genome at the chromatin level and provides an example of the impact of a single transcription factor on a whole plant genome.

Background & Summary

Basic leucine zipper11 (bZIP11) is a transcription factor (TF) which regulates gene expression during low-energy conditions in plants and enables plants to adjust their metabolism, growth, and development to such unfavourable conditions[1–3]. In *Arabidopsis thaliana* (Arabidopsis), bZIP11 belongs to a group of five proteins involved in sugar responses, named the S_1 bZIP group[2,4–8]. It is estimated by DNA Affinity Purification with high throughput sequencing (DAP-seq) that bZIP11 contains DNA-binding sites in over 7,000 genes in Arabidopsis, which is nearly one third of the entire genes in the genome[9]. The bZIP TFs bind DNA at *cis*-regulatory elements (CREs) known as G-boxes, which all have a conserved ACGT core flanked by cytosines or guanines (C/GACGTG/C)[10]. bZIP11 has been demonstrated to promote the expression of specific auxin-related genes by recruiting histone acetylation machinery to enhance chromatin accessibility[3,11]. However, the extent to which bZIP11 impacts chromatin accessibility at the whole-genome scale remains unknown.

Assay for Transposase-Accessible Chromatin with high throughput sequencing (ATAC-seq) is a technique which can determine genome-wide locations of chromatin accessible to transposase insertion and by extension, other proteins, for example TFs[12,13]. This technique is rapid and can be performed on small quantities of starting material. Previous studies have performed ATAC-seq on different plant organs, conditions, or in response to different treatments to determine changes in accessibility of those DNA regions that are likely to contain regulatory sequences[14–17]. Here we report ATAC-seq results in response to induction of a single plant TF, with known regulatory sequences, to determine the genome-wide effect of this TF on chromatin accessibility in Arabidopsis.

[1]School of Biological Sciences, The University of Queensland, St Lucia, QLD, 4072, Australia. [2]ARC Centre for Plant Success in Nature and Agriculture, The University of Queensland, St Lucia, QLD, 4072, Australia. [3]School of Natural Sciences, University of Tasmania, Hobart, Tasmania, Australia. [4]Institute for Plant Biochemistry, Heinrich Heine University, Dusseldorf, Germany. ✉e-mail: a.hellens@uq.net.au; francois.barbier@uq.edu.au

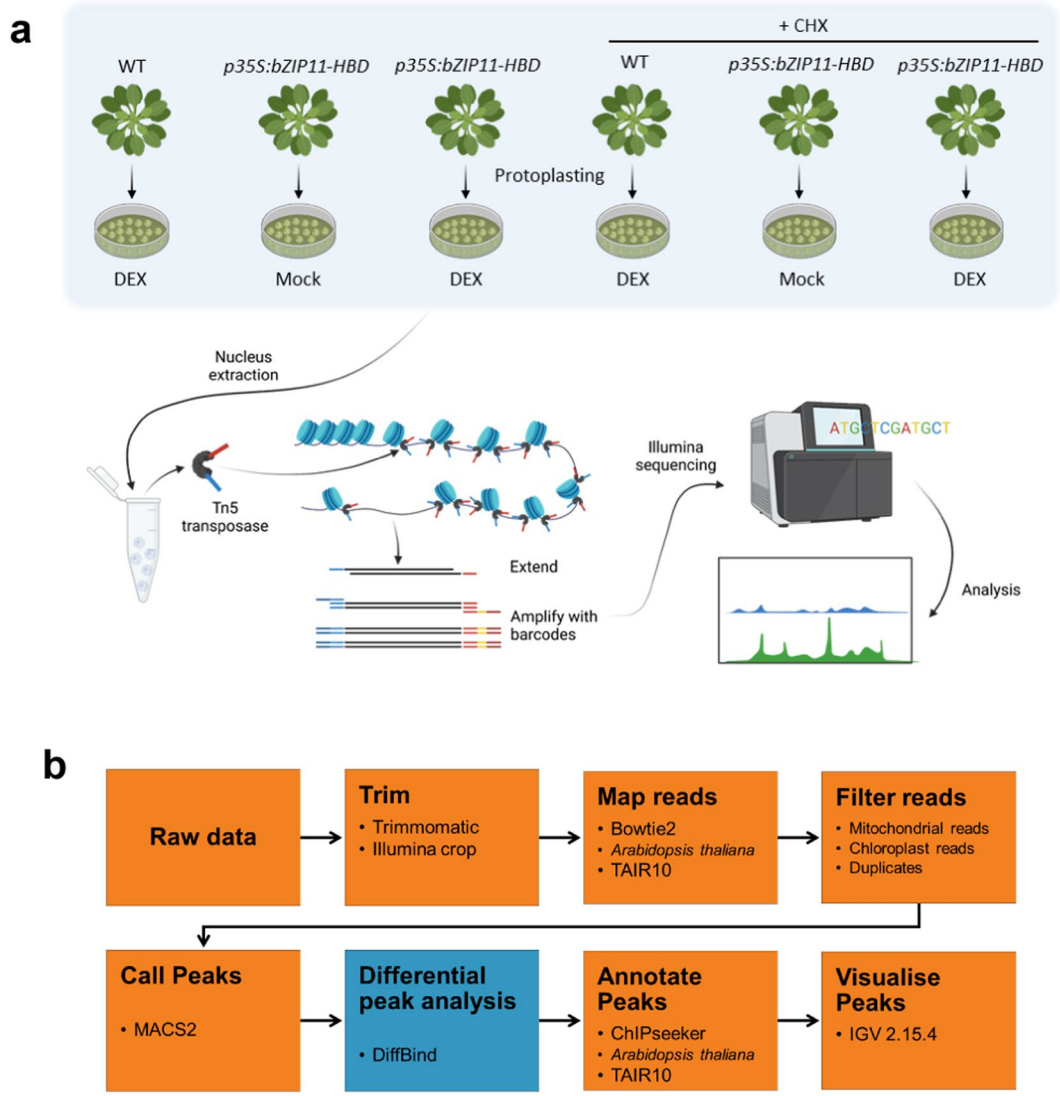

Fig. 1 Overview of experimental design and data analysis workflow. (**a**) Experimental design and ATAC-seq library preparation. Arabidopsis protoplasts of four-week-old wild type (Col-0) or *p35S:bZIP11-HBD* were isolated. Protoplasts were then treated with different combinations of 10 µM dexamethasone, acetone, water, and 35 µM of cycloheximide (CHX). Each condition was carried out in four biological replicates. After nucleus extraction, samples were incubated with a hyperactive Tn5 transposase which adds adapters onto the DNA. DNA regions were amplified using primers against the adapters, so only accessible regions are amplified. PCR also added sequencing barcodes allowing for samples to be pooled and sent for sequencing. (**a**) was adapted from Buenrostro *et al.*, 2015. (**b**) The analysis workflow of ATAC-seq orange boxes indicate step was carried out using Galaxy Australia. Blue indicates step was carried out in R.

To achieve a comprehensive profile of accessible chromatin regions and discover new downstream targets of bZIP11, we generated 24 chromatin accessibility data sets from wild-type (WT) Arabidopsis protoplast samples, as well as from transgenic *p35S:bZIP11-HBD* Arabidopsis plants[18]. In these *p35S:bZIP11-HBD* plants, the expression of *bZIP11* coding sequence is driven by the cauliflower mosaic virus, *CaMV35S*, promoter (*p35S*) that leads to ectopic gene expression in the whole plant. A rat glucocorticoid receptor, or hormone binding domain (HBD), is fused to bZIP11, and retains this TF in the cytoplasm. Upon treatment with dexamethasone (DEX), which binds to the HBD, the translocation of bZIP11 to the nucleus is enabled, allowing its TF activity to occur[19]. Four-week-old Arabidopsis plants were used to extract leaf protoplasts from approximately six leaves per plant (experiment summarised in Fig. 1a). Protoplasts were treated for 45 minutes after a one hr recovery period following protoplast extraction. Four biological replicates were treated with either DEX, which induces the translocation of bZIP11 protein into the nucleus, or acetone, the solvent for DEX (Mock control). Using protoplasts allows for a rapid and homogeneous chemical uptake which reduces variability between samples[20]. In parallel, the samples were treated, prior to DEX or acetone treatment, with cycloheximide (CHX), a protein biosynthesis inhibitor[21] that enables to discriminate the direct targets of bZIP11 from its indirect targets. Approximately 50,000 cells from each replicate of each treatment were used for ATAC-seq. In total,

Genotype	Treatment	Sample ID	Raw Reads	Clean Reads	Mapped Reads	Called Peaks	Accession	DiffBound Peaks
Col -0	Dex	AH025	14,017,763	11,559,584	7,335,921	19,874	SAMN34226419	10,140 (8,843 genes)
Col -0	Dex	AH028	10,143,097	7,007,692	4,925,970	18,618	SAMN34226420	
Col -0	Dex	AH027	11,313,278	7,305,956	4,891,108	19,857	SAMN34226421	
Col -0	Dex	AH028	9,972,594	6,476,678	4,631,287	19,814	SAMN34226422	
35 S:bZIP11 -HBD	Mock	AH029	23,738,704	8,984,170	6,593,699	19,301	SAMN34226423	11,236 (9,664 genes 3339 gained 2518 lost)
35 S:bZIP11 -HBD	Mock	AH030	23,487,379	19,317,810	11,256,808	21,167	SAMN34226424	
35 S:bZIP11 -HBD	Mock	AH031	11,564,134	8,689,856	6,144,551	20,210	SAMN34226425	
35 S:bZIP11 -HBD	Mock	AH032	10,904,533	5,642,758	4,334,768	19,474	SAMN34226426	
35 S:bZIP11 -HBD	Dex	AH033	51,908,821	31,990,286	16,607,717	21,979	SAMN34226427	
35 S:bZIP11 -HBD	Dex	AH034	22,101,174	21,768,988	12,416,405	22,757	SAMN34226428	
35 S:bZIP11 -HBD	Dex	AH035	26,803,740	25,482,872	14,052,875	22,081	SAMN34226429	
35 S:bZIP11 -HBD	Dex	AH036	26,846,853	24,840,140	13,471,482	22,638	SAMN34226430	
Col - 0	CHX + dex	AH037	8,242,523	5,100,362	3,816,207	18,200	SAMN34226431	8,154 (6,689 genes)
Col - 0	CHX + dex	AH038	9,959,240	6,938,240	4,974,236	18,479	SAMN34226432	
Col - 0	CHX + dex	AH039	22,104,359	11,316,082	7,326,410	21,035	SAMN34226433	
Col - 0	CHX + dex	AH040	20,066,853	11,752,986	7,625,434	20,872	SAMN34226434	
35 S:bZIP11 -HBD	CHX + mock	AH041	11,576,489	7,333,816	5,443,565	19,553	SAMN34226435	11,483 (8,967 genes 2,021 lost 4,319 gained)
35 S:bZIP11 -HBD	CHX + mock	AH042	9,287,775	5,451,356	4,190,938	17,891	SAMN34226436	
35 S:bZIP11 -HBD	CHX + mock	AH043	13,856,888	8,288,610	6,010,492	20,168	SAMN34226437	
35 S:bZIP11 -HBD	CHX + mock	AH044	7,820,098	6,459,694	4,927,170	18,343	SAMN34226438	
35 S:bZIP11 -HBD	CHX + dex	AH045	32,518,073	15,864,764	9,527,833	22,393	SAMN34226439	
35 S:bZIP11 -HBD	CHX + dex	AH046	32,036,847	28,842,408	15,347,729	22,072	SAMN34226440	
35 S:bZIP11 -HBD	CHX + dex	AH047	15,953,569	13,695,372	8,699,347	21,386	SAMN34226441	
35 S:bZIP11 -HBD	CHX + dex	AH048	23,280,510	20,464,908	11,939,899	22,177	SAMN34226442	

Table 1. Summary of ATAC-seq sequencing, mapping, and peak calling. DiffBound peaks were determined by comparing bZIP11-induced samples with each control (WT + Dex treated and bZIP11-inducibe + Mock treated) for both with and without CHX.

approximately 10,000 regions of the genome were determined as differentially accessible regions (DARs) upon induction of bZIP11 translocation to the nucleus, depending on which control was used (Table 1). These DARs are summarised by a core list of 2,553 genes identified to have their chromatin accessibility directly influenced by bZIP11.

Methods

Plant materials. *Arabidopsis thaliana* seeds were stratified for three days at four degrees Celsius then transferred to growth chambers with 16 h light: 8 h dark, 22 °C day: 20 °C night with 150 ± 20 µmol m^{-2} s^{-1} light intensity. Plants were grown in UQ23 potting mix (70% composted pine bark (zero to five mm), 30% cocopeat, supplemented with dolomite and osmocote).

Protoplast isolation. Four-week-old wild type (WT) Columbia-0 (Col-0) and inducible bZIP11 (*p35S:bZIP11-HBD*)[18] plants were used to extract mesophyll protoplasts via the epidermal leaf peel method[22]. Six leaves were placed in 10 mL of enzyme solution (1% Cellulase 'Onozuka' R10, 0.25% maceroenzyme 'Onozuka' R10, 0.4 M mannitol, 20 mM KCl, 20 mM MES, 10 mM CaCl2, 0.1% BSA, adjust to pH 5.7) and digested for 1 h with constant gentle agitation. Cells were filtered through 50 µM mesh (CellTrics, Sysmex, Norderstedt, Germany) then washed twice in W5 (154 mM NaCl, 125 mM $CaCl_2$, 5 mM KCl, 2 mM MES). Protoplasts were then re-suspended in MMg (0.4 M mannitol, 15 mM $MgCl_2$, 4 mM MES, adjust to pH 5.7) at a concentration of 200,000 cells per mL. Reactions took place in 2 mL, in six-well plastic plates with constant agitation. WT cells were treated with 10 µM DEX, Mock plants were treated with acetone, and bZIP11-inducible plants were treated with 10 µM DEX. For CHX-treated reactions, CHX was added prior to DEX or acetone treatment at a concentration of 35 µM. 45 min after treatment, cells were collected by centrifugation and resuspended at a concentration of approximately 50,000 cells per sample.

RNA extraction and gene expression. Total RNA was extracted (NucleoSpin RNA Extraction, MACHEREY-NAGEL, Düren, Germany), reverse transcribed into cDNA (iScript Supermix, Bio-Rad Laboratories, California, USA), and diluted cDNA was used as a template for quantitative Real-Time PCR (SensiFASTTM SYBR® No-ROX Kit from Bioline) according to manufacturer's instructions. Fluorescence was measured using a CFX384 TouchTM Real-Time PCR Detection System (Bio-Rad Laboratories, California, USA) using the following protocol: 95 °C for 3 min, 40 cycles at 10 s each for 95 °C and 59 °C for 45 s, and 1 min each for 95 °C and 55 °C. The ΔΔCt technique was used to determine gene expression and primer efficiency was used to correct it. The geomean expression of two technical replicates of each, *TUBULIN3* (At5g62700), *ACTIN* (Combination of *ACT2*, *ACT7*, and *ACT8*: At3Gg18780, At5g09810, and At1g49240), and *18 S* (18 S rRNA) were used to normalise gene expression. Every primer sequence used in this study is outlined in Supplementary Table 1.

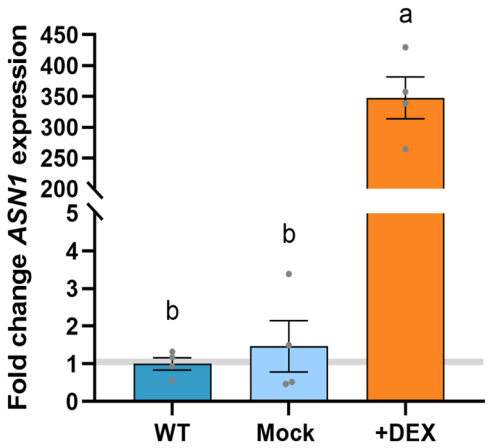

Fig. 2 Validation of bZIP11 activity induction. Expression of the bZIP11 direct target *ASN1* in response to DEX treatment, Data are mean ± s.e.m (n = 4). Letters on the graph indicate statistical differences determined by one-way ANOVA using Tukey correction for multiple comparisons.

ATAC-seq protocol. ATAC-seq library preparation was performed as modified from Buenrostro *et al.*[12,13,23]. Following protoplast extraction, nuclei were isolated from approximately 50,000 cells per reaction by sucrose sedimentation, using a method modified from Bajic *et al.*[14]. Freshly extracted cells were centrifuged at 500 × g at 4 °C. The following steps were all carried out on ice. Supernatant was discarded and pellet was resuspended in 1 mL of ice-cold nuclei purification buffer (20 mM MOPS, 40 mM NaCl, 90 mM KCl, 2 mM EDTA, 0.5 mM EGTA, 0.5 mM spermidine, 0.2 mM spermine 1 × protease inhibitors, adjust to pH 7). Cells were then filtered through 30 μM mesh (CellTrics, Sysmex, Norderstedt, Germany). Nuclei were then spun down at 1200 × g for 10 min at 4 °C and pellet was resuspended in 1 mL of ice-cold nuclei extraction buffer 2 (0.25 m sucrose, 10 mM Tris-HCl pH8, 10 mM MgCl, 1% Triton X-100, 1 × protease inhibitors). This step was repeated but this time pellet was resuspended in 300 μL of NPB and this resuspension of nuclei was carefully layered over 300 μL of ice-cold nuclei extraction buffer 3 (1.7 M sucrose, 10 mM Tris-HCl pH 8, 2 mM MgCl, 0.15% Triton X-100 1 × protease inhibitor). The two layers were then spun down at 300 × g for 20 min at 4 °C following which, supernatant was removed. Nuclei were resuspended in 50 μL of tagmentation reaction mix, as per manufacturer instructions (TDE1, Illumina) and incubated at 37 °C for 30 min with gentle agitation every 5 min. Reactions were purified following manufacturer's instructions using a QIAGEN MinElute PCR purification kit (catalogue number 28004) and eluted in 11 μL of elution buffer. DNA was amplified by PCR using ATAC barcoded primers and NEB Next High-Fidelity PCR Master Mix (5 min 72 °C, 30 sec. 98 °C, then 5 × (10 sec. 98 °C, 30 sec. 63 °C, 1 min 72 °C) held at 4 °C). 5 μL of the PCR reaction was then further amplified by quantitative PCR (qPCR) (30 sec. 98 °C, then 20 × (10 sec. 98 °C, 30 sec. 63 °C, 1 min 72 °C)) to determine the required number of additional cycles. Additional cycle number for each reaction was determined by the cycle number for which a reaction has reached one third of its maximum, using the linear fluorescence vs cycle number graph from the qPCR. All libraries were purified with AMPure XP beads at a ratio of 1.5:1 beads:PCR reaction. Final elution in 20 μL of 10 mM Tris pH 8. Libraries were sequenced using Illumina HiSeq paired end 150 bp by NovoGene, Singapore.

ATAC-seq data analysis. A summary of the ATAC-seq data analysis workflow used in this study is represented in Fig. 1b. Processing was carried out using Galaxy Australia[24] and R with RStudio (Version 4.2.2) with the following steps. In Galaxy, raw reads were trimmed using Trimmomatic[25] with the following settings: a 10 bp HEADCROP, a SLIDINGWINDOW with an average quality of 30 over every 6 bp, and an ILLUMINACLIP NexteraPE. Reads shorter than 30 bp and longer than 1000 bp were discarded. Reads were mapped against *Arabidopsis thaliana* TAIR10 reference genome (https://www.arabidopsis.org) using Bowtie2[26], with paired end, dovetailing, and a maximum fragment length of 1000. Reads smaller than 30 bp, duplicate reads, reads with a quality score of <30 phred, and those which were mapped to the chloroplast or mitochondrial genome were discarded. Peaks were called with MACS2[27], using the inputs: single-end BED, effective genome size 1.2e8, an extension size of 200 and a shift size of 100. BED and BAM and index files were then imported into RStudio and DARs were determined using the package DiffBind[28]. Peaks were read with peakCaller = "narrow", minOverlap = 3 and dba.contrast function was specified to compare bZIP11-induced samples to either WT or Mock-treated samples. The package rtracklayer was used to convert the DARs determined by DiffBind into BED format. The peaks report was then imported back into Galaxy where differential peaks were annotated to the Arabidopsis reference genome using ChIPseeker[29]. The coordinates of peaks were compared with the annotated genome to determine the distribution of the peaks. ChIPseeker was also used to retrieve the nearest genes around differentially accessible peaks between the treatments. The resulting BED file of annotated DARs was imported into the Interactive Genome Viewer (Broad Institute, University of California)[30] along with BED files DARs from MACS2 output for visualisation. STREME[31] from the MEME suite was used to identify overrepresented motifs in the DAR sequences (minimum width = 4, maximum width = 15, p-value threshold = 0.05). Overrepresented motifs were then compared with DAP-seq motifs[9] using TOMTOM[32] to search for motifs overlapping by at least 5 bp.

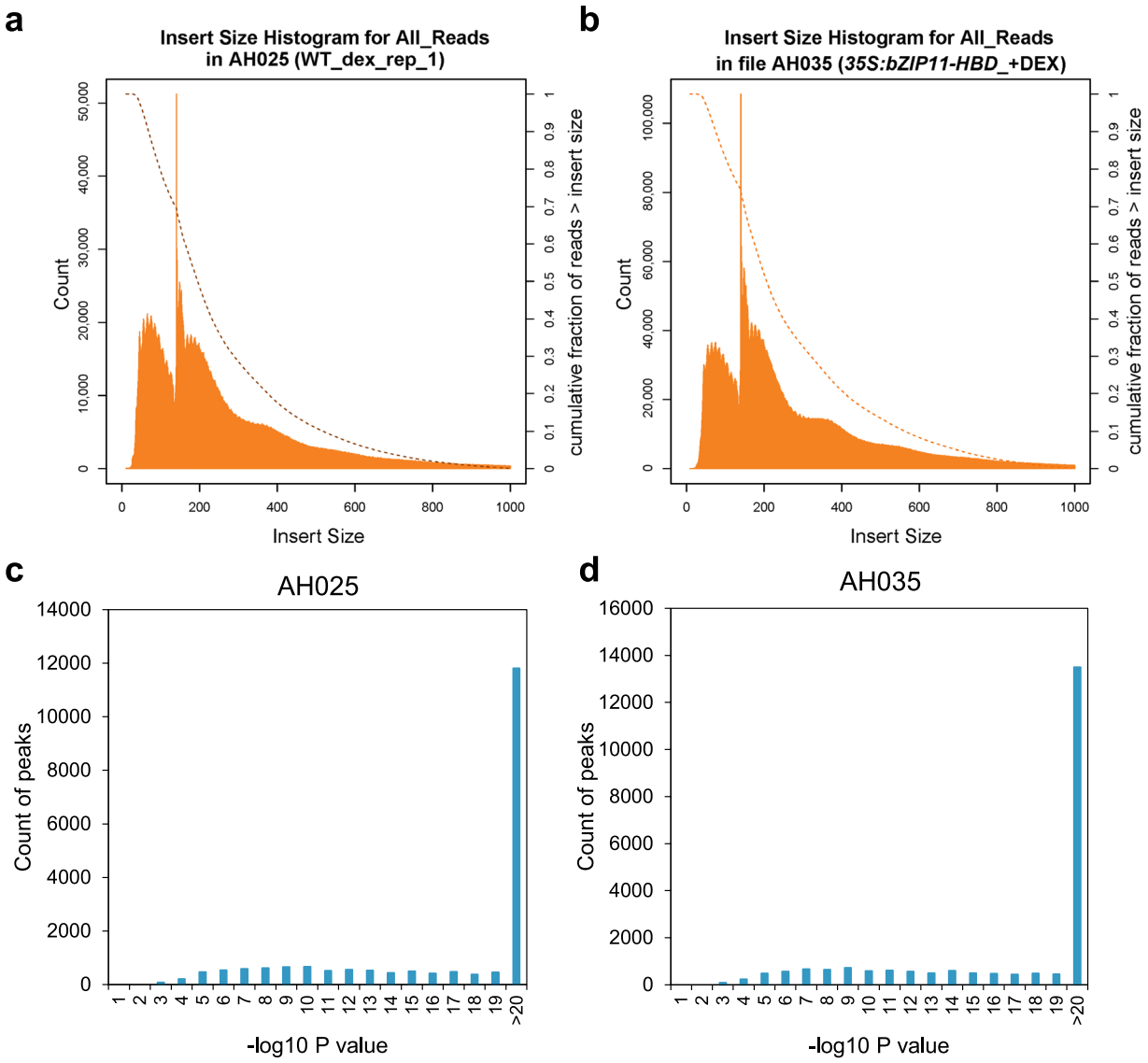

Fig. 3 Quality metrics of ATAC-seq reads. (**a,b**) Fragment size distribution of ATAC-seq reads for two representative samples: sample AH025 and AH035 respectively. (**c,d**) Peak score (-log10 (P-value)) distribution for representative samples: sample AH025 (**c**) and AH035 (**d**).

Data Records

ATAC-seq reads and peak files have been submitted to the National Center for Biotechnology Information Sequence Read Archive (NCBI SRA, PRJNA956597)[33]. https://trace.ncbi.nlm.nih.gov/Traces/?view=study&acc=SRP433061.

Technical Validation

To validate the induction of bZIP11 activity upon DEX treatment, we measured the expression of *ASPARAGINE SYNTHASE1* (*ASN1*), a known direct target of this TF[18]. *ASN1* expression was nearly 350-fold upregulated in the DEX-treated *p35S:bZIP11-HBD* samples compared to the DEX-treated WT samples and the Mock-treated *p35S:bZIP11-HBD* samples (Fig. 2), confirming that DEX treatment efficiently induced bZIP11 activity in the *p35S:bZIP11-HBD* samples.

We then evaluated the quality and content of the entire ATAC-seq dataset. Most reads were less than 150 bp, consistent with being shorter than one nucleosome (Fig. 3a,b)[34] and most peaks showed a -log10 P-value score greater than 20, indicating the low likelihood of the peak calling occurring by chance (Fig. 3c,d). Samples where bZIP11 was induced cluster together in a hierarchical ranking plot, depicted by orange (-CHX) and red (+CHX) samples (Fig. 4a). Using differentially accessible peaks, we plotted chromatin accessible signals around genes in response to bZIP11 induction. The regions around transcription start sites are enriched, which is expected for a TF (Fig. 4b). Over 90% of DARs are found in promotor regions of genes, which is expected for a small genome like Arabidopsis (Fig. 4c). In addition, the DAR sequences identified in response to bZIP11 induction, both with and without CHX, were found to be highly enriched in the bZIP CRE, G-box motif (Fig. 4d).

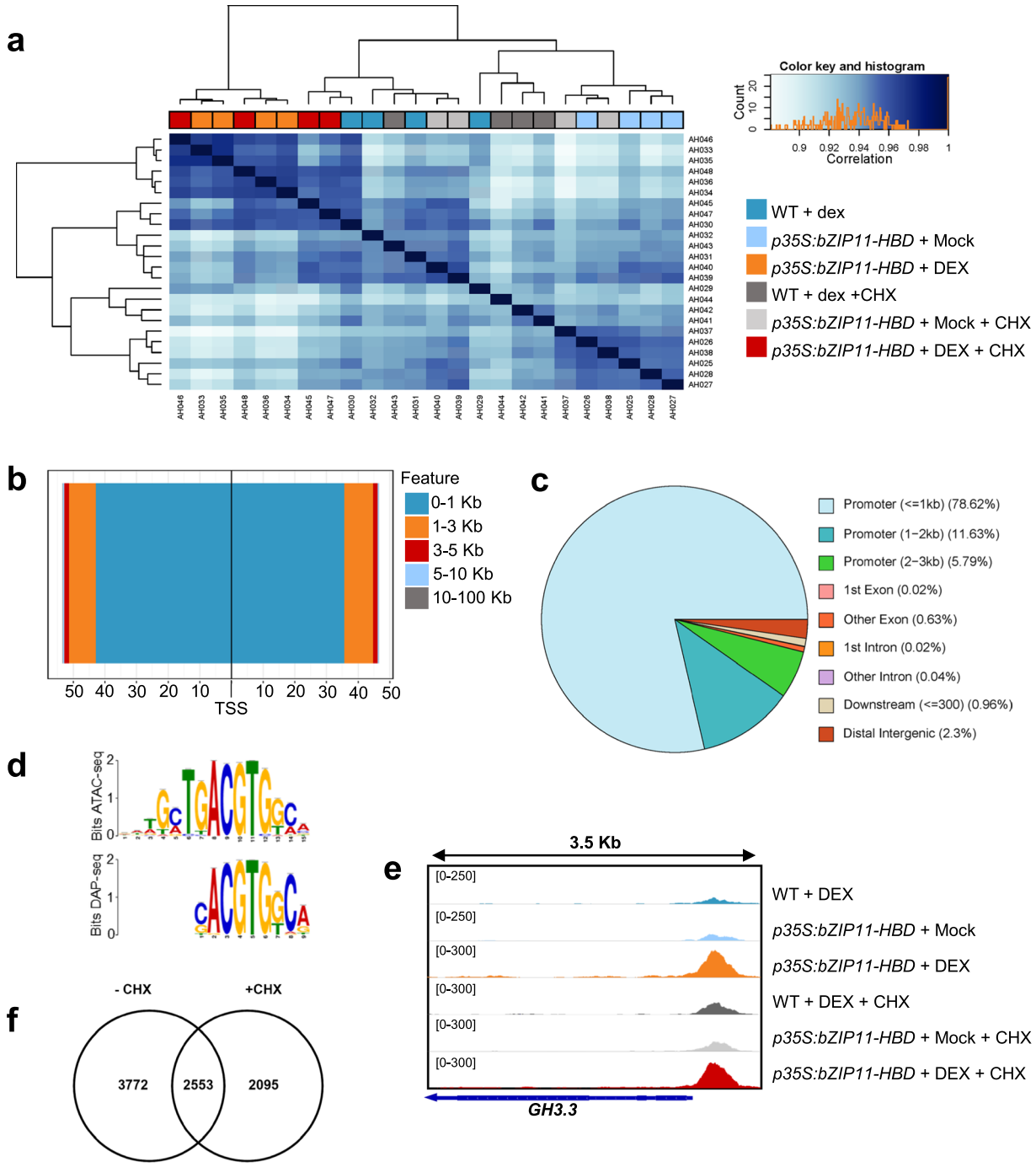

Fig. 4 Features of ATAC-seq peaks identified in this dataset. (**a**) Hierarchical clustering of samples based on sample genotype, treatment and replicate number. (**b**) Schematic representation of the distribution of DAR positions upstream and downstream from the TSS of the nearest annotated genes. (**c**) DAR Classification into genic region, based on their location to the nearest gene. (**d**) Motif enrichment analysis obtained in this ATAC-seq (top logo) compared to motif enrichment obtained from DAP-seq data (bottom logo). (**e**) Genome browser views showing chromatin accessibility around *GH3.3* locus in response to bZIP11 in different samples of this experiment. (**f**) Overlap of differentially accessible regions (DARs) determined when bZIP11 induced samples were compared to both wild type (WT) and Mock-treated samples both without cycloheximide (-CHX bubble) and with CHX (-CHX bubble).

This motif closely resembles to the motif identified through DNA Affinity Purification and sequencing (DAP-seq) in response to bZIP11 (Fig. 4d)[9], supporting that these DARs are regulated by bZIP11. Finally, we tested whether bZIP11 induction efficiently made chromatin more accessible on expected targets. To do so, we visualised the result of the ATAC-seq on *GH3.3* locus, known to be directly regulated at the chromatin level by bZIP11[11]. The results indicate that the chromatin is more accessible when bZIP11 is induced in the

p35S:bZIP11-HBD samples in absence or presence of CHX (Fig. 4e), consistent with the fact that bZIP11 regulates *GH3.3* at the chromatin level and that the induction of bZIP11 successfully regulated chromatin accessibility in this experiment. Altogether, these data indicate that bZIP11 regulates chromatin to enhance the accessibility of *cis* elements to *trans* regulatory factors, and that this regulatory mechanism concerns a large portion of bZIP11 targets.

To validate direct bZIP11-induced regions of chromatin accessibility, this experiment was repeated both with and without CHX. Without CHX, ATAC-seq determined 10,140 bZIP11-induced DARs, compared to WT, and 11,236 DARs, compared to Mock-treated samples (Table 1). Using ChIPseeker[29], non CHX DARs were mapped to 6,325 genes (Supplementary Fig. 1a). In the presence of CHX, ATAC-seq determined 8,154 bZIP11-induced DARs, compared to WT, and 11,483 DARs, compared to Mock-treated samples (Table 1). With CHX, DARs were mapped to 4,649 genes (Supplementary Fig. 1b). There are fewer genes made accessible in the presence of CHX, indicating that the treatment worked. Interestingly, in the presence of CHX, there are 3,772 lost genes and 2,095 gained genes (Fig. 4f). This is expected as often multiple proteins are required for both increasing and decreasing chromatin accessibility. To determine which genes are likely to be made accessible directly by bZIP11, the genes corresponding to DARs in CHX-treated and non-treated samples were compared (Fig. 4f). Genes which were annotated in both data sets provide a list of 2,553 genes which are likely to have chromatin accessibility regulated by bZIP11 directly (Supplementary Table 2).

Code availability

All codes used for this study are available on GitHub (https://github.com/AliciaHellens/bZIP11_ATAC-seq).

Received: 4 May 2023; Accepted: 17 July 2023;
Published online: 27 July 2023

References

1. Fichtner, F., Dissanayake, I. M., Lacombe, B. & Barbier, F. Sugar and Nitrate Sensing: A Multi-Billion-Year Story. *Trends in Plant Science* **26**, 352–374 (2021).
2. Dröge-Laser, W. & Weiste, C. The C/S1 bZIP Network: A Regulatory Hub Orchestrating Plant Energy Homeostasis. *Trends in Plant Science* **23**, 422–433 (2018).
3. Pedrotti, L. *et al*. Snf1-RELATED KINASE1-Controlled C/S1-bZIP Signaling Activates Alternative Mitochondrial Metabolic Pathways to Ensure Plant Survival in Extended Darkness. *The Plant Cell* **30**, 495–509 (2018).
4. Wiese, A., Elzinga, N., Wobbes, B. & Smeekens, S. A Conserved Upstream Open Reading Frame Mediates Sucrose-Induced Repression of Translation. *Plant Cell* **16**, 1717–1729 (2004).
5. Wielopolska, A., Townley, H., Moore, I., Waterhouse, P. & Helliwell, C. A high-throughput inducible RNAi vector for plants. *Plant Biotechnology Journal* **3**, 583–590 (2005).
6. Hummel, M., Rahmani, F., Smeekens, S. & Hanson, J. Sucrose-mediated translational control. *Ann Bot* **104**, 1–7 (2009).
7. Yamashita, Y. *et al*. Sucrose sensing through nascent peptide-meditated ribosome stalling at the stop codon of Arabidopsis bZIP11 uORF2. *FEBS Letters* **591**, 1266–1277 (2017).
8. Dröge-Laser, W., Snoek, B. L., Snel, B. & Weiste, C. The Arabidopsis bZIP transcription factor family—an update. *Current Opinion in Plant Biology* **45**, 36–49 (2018).
9. O'Malley, R. C. *et al*. Cistrome and Epicistrome Features Shape the Regulatory DNA Landscape. *Cell* **165**, 1280–1292 (2016).
10. Jakoby, M. *et al*. bZIP transcription factors in Arabidopsis. *Trends in Plant Science* **7**, 106–111 (2002).
11. Weiste, C. & Dröge-Laser, W. The Arabidopsis transcription factor bZIP11 activates auxin-mediated transcription by recruiting the histone acetylation machinery. *Nat Commun* **5**, 3883 (2014).
12. Buenrostro, J. D., Giresi, P. G., Zaba, L. C., Chang, H. Y. & Greenleaf, W. J. Transposition of native chromatin for multimodal regulatory analysis and personal epigenomics. *Nat Methods* **10**, 1213–1218 (2013).
13. Buenrostro, J. D., Wu, B., Chang, H. Y. & Greenleaf, W. J. ATAC-seq: A Method for Assaying Chromatin Accessibility Genome-Wide. *Current Protocols in Molecular Biology* **109**, 21.29.1–21.29.9 (2015).
14. Bajic, M., Maher, K. A. & Deal, R. B. Identification of Open Chromatin Regions in Plant Genomes Using ATAC-Seq. in *Plant Chromatin Dynamics: Methods and Protocols* (eds. Bemer, M. & Baroux, C.) 183–201, https://doi.org/10.1007/978-1-4939-7318-7_12 (Springer New York, 2018).
15. Maher, K. A. *et al*. Profiling of Accessible Chromatin Regions across Multiple Plant Species and Cell Types Reveals Common Gene Regulatory Principles and New Control Modules. *The Plant Cell* **30**, 15–36 (2018).
16. Potter, K. C., Wang, J., Schaller, G. E. & Kieber, J. J. Cytokinin modulates context-dependent chromatin accessibility through the type-B response regulators. *Nature Plants* **4**, 1102 (2018).
17. Tian, H. *et al*. Photoperiod-responsive changes in chromatin accessibility in phloem companion and epidermis cells of Arabidopsis leaves. *The Plant Cell* **33**, 475–491 (2021).
18. Hanson, J., Hanssen, M., Wiese, A., Hendriks, M. M. W. B. & Smeekens, S. The sucrose regulated transcription factor bZIP11 affects amino acid metabolism by regulating the expression of ASPARAGINE SYNTHETASE1 and PROLINE DEHYDROGENASE2. *The Plant Journal* **53**, 935–949 (2008).
19. Aoyama, T. & Chua, N. H. A glucocorticoid-mediated transcriptional induction system in transgenic plants. *Plant J* **11**, 605–612 (1997).
20. Yoo, S.-D., Cho, Y.-H. & Sheen, J. Arabidopsis mesophyll protoplasts: a versatile cell system for transient gene expression analysis. *Nat Protoc* **2**, 1565–1572 (2007).
21. Obrig, T. G., Culp, W. J., McKeehan, W. L. & Hardesty, B. The Mechanism by which Cycloheximide and Related Glutarimide Antibiotics Inhibit Peptide Synthesis on Reticulocyte Ribosomes. *Journal of Biological Chemistry* **246**, 174–181 (1971).
22. Wu, F.-H. *et al*. Tape-Arabidopsis Sandwich - a simpler Arabidopsis protoplast isolation method. *Plant Methods* **5**, 16 (2009).
23. Humphreys, J. L., Beveridge, C. & Tanurdzic, M. Strigolactone-dependent gene regulation requires chromatin remodeling. Preprint at https://doi.org/10.1101/2023.02.25.529999 (2023).
24. The Galaxy Community. The Galaxy platform for accessible, reproducible and collaborative biomedical analyses: 2022 update. *Nucleic Acids Research* **50**, W345–W351 (2022).
25. Bolger, A. M., Lohse, M. & Usadel, B. Trimmomatic: a flexible trimmer for Illumina sequence data. *Bioinformatics* **30**, 2114–2120 (2014).
26. Langmead, B. & Salzberg, S. L. Fast gapped-read alignment with Bowtie 2. *Nat Methods* **9**, 357–359 (2012).
27. Zhang, Y. *et al*. Model-based Analysis of ChIP-Seq (MACS). *Genome Biology* **9**, R137 (2008).
28. Stark, R. & Brown, G. DiffBind: differential binding analysis of ChIP-Seq peak data. *R package version* **100** (2011).

29. Yu, G., Wang, L.-G. & He, Q.-Y. ChIPseeker: an R/Bioconductor package for ChIP peak annotation, comparison and visualization. *Bioinformatics* **31**, 2382–2383 (2015).
30. Robinson, J. T. *et al*. Integrative genomics viewer. *Nat Biotechnol* **29**, 24–26 (2011).
31. Bailey, T. L. STREME: accurate and versatile sequence motif discovery. *Bioinformatics* **37**, 2834–2840 (2021).
32. Gupta, S., Stamatoyannopoulos, J. A., Bailey, T. L. & Noble, W. S. Quantifying similarity between motifs. *Genome Biology* **8**, R24 (2007).
33. Hellens, AM. SRP433061, *NCBI Sequence Read Archive*, https://identifiers.org/ncbi/insdc.sra:SRP433061 (2023).
34. Clark, D. J. Nucleosome Positioning, Nucleosome Spacing and the Nucleosome Code. *J Biomol Struct Dyn* **27**, 781–793 (2010).

Acknowledgements

Christine Beveridge is the recipient of an Australian Research Council Centre of Excellence CE200100015 and an Australian Laureate Fellowship FL180100139. Alicia Hellens is supported by a Commonwealth Scientific and Industrial Research Organization Postgraduate Scholarship. Figure 1a was made with biorender.com.

Author contributions

Experiments were designed by all authors. Experiments were carried out by A.H., J.H., F.F. and F.B. Data were analysed by all authors. A.H. and F.B. wrote the manuscript. All authors commented and approved the final version of the manuscript.

Competing interests

The authors declare no competing interests.

Additional information

Supplementary information The online version contains supplementary material available at https://doi.org/10.1038/s41597-023-02395-6.

Correspondence and requests for materials should be addressed to A.M.H. or F.F.B.

Reprints and permissions information is available at www.nature.com/reprints.

Publisher's note Springer Nature remains neutral with regard to jurisdictional claims in published maps and institutional affiliations.

Open Access This article is licensed under a Creative Commons Attribution 4.0 International License, which permits use, sharing, adaptation, distribution and reproduction in any medium or format, as long as you give appropriate credit to the original author(s) and the source, provide a link to the Creative Commons license, and indicate if changes were made. The images or other third party material in this article are included in the article's Creative Commons license, unless indicated otherwise in a credit line to the material. If material is not included in the article's Creative Commons license and your intended use is not permitted by statutory regulation or exceeds the permitted use, you will need to obtain permission directly from the copyright holder. To view a copy of this license, visit http://creativecommons.org/licenses/by/4.0/.

© The Author(s) 2023